# Supramolecular structure in the membrane of *Staphylococcus aureus*

Jorge García-Lara[a,1], Felix Weihs[a], Xing Ma[a,2], Lucas Walker[a], Roy R. Chaudhuri[a], Jagath Kasturiarachchi[a,3], Howard Crossley[a], Ramin Golestanian[b,4], and Simon J. Foster[a,4]

[a]The Krebs Institute, Department of Molecular Biology and Microbiology, University of Sheffield, Sheffield S10 2TN, United Kingdom; and [b]Rudolf Peierls Centre for Theoretical Physics, University of Oxford, Oxford OX1 3NP, United Kingdom

Edited by Richard P. Novick, New York University School of Medicine, New York, NY, and approved October 28, 2015 (received for review May 20, 2015)

**All life demands the temporal and spatial control of essential biological functions. In bacteria, the recent discovery of coordinating elements provides a framework to begin to explain cell growth and division. Here we present the discovery of a supramolecular structure in the membrane of the coccal bacterium *Staphylococcus aureus*, which leads to the formation of a large-scale pattern across the entire cell body; this has been unveiled by studying the distribution of essential proteins involved in lipid metabolism (PlsY and CdsA). The organization is found to require MreD, which determines morphology in rod-shaped cells. The distribution of protein complexes can be explained as a spontaneous pattern formation arising from the competition between the energy cost of bending that they impose on the membrane, their entropy of mixing, and the geometric constraints in the system. Our results provide evidence for the existence of a self-organized and nonpercolating molecular scaffold involving MreD as an organizer for optimal cell function and growth based on the intrinsic self-assembling properties of biological molecules.**

membrane | model | staphylococcus | MreD | PlsY

The perpetuation of all cellular life requires the temporal and spatial management of essential biological functions, within the morphological framework characteristic of a specific organism. The underlying processes, which determine cell shape, are intimately intertwined with cell division and constitute pivotal issues for cell biology; their coordination in prokaryotes is mediated through counterparts of eukaryotic actin, tubulin, and intermediate filaments in addition to other specific components (1, 2). Several of these apparent cytoskeletal elements capitalize on their membrane binding properties, assembling along the longitudinal axis, between the poles of rod-shaped cells; they participate in many processes, including selection of the division site via the Min system and other components (3, 4); guidance and control of the cell wall biosynthetic machinery responsible for cell size, polarity, and shape through the actin-like protein MreB (5–11); and chromosome partitioning into daughter cells using another actin-like filament, ParM (12).

Despite this set of highly coordinated mechanisms, it has recently been shown that otherwise rod- and cocci-shaped bacteria can exist as largely spherical wall-less forms known as L-forms, with the capacity to divide (13). Importantly, the division of L-forms of the rod-shaped bacterium *Bacillus subtilis* is freed from the requirement of the classical tubulin-like division component FtsZ (14). L-forms appear to divide by scission after blebbing, tabulation, or vesiculation dependent on an altered rate of membrane biosynthesis (15); this harks back perhaps to a more evolutionary primitive mechanism permitting cellular proliferation. Thus, are there underlying organizational mechanisms that exist, independent of apparent cytoskeletal elements? The fluid mosaic model proposing the free diffusion of membrane proteins through the lipids has been challenged by growing evidence of the subcellular heterogeneity within the membrane resulting from diverse clustering of lipids and proteins (16–18).

Membrane curvature can act as a cue for localization of components (16). Raft aggregation of transmembrane proteins and the presence of compartment boundaries are insufficient explanations for such patterning. The physiological principles and molecular processes governing pattern formation are largely unknown.

*Staphylococcus aureus* is a coccal bacterium that can grow and divide in three consecutive orthogonal planes with fidelity (19); however, it lacks key morphogenetic components, such as MinCDE and MreB (20). Hence, what are the spatial organizers in *S. aureus* (21)?

Here we present the discovery of a supramolecular structure in the membrane of *S. aureus* that has been unveiled by studying the distribution of essential proteins involved in lipid metabolism (PlsY and CdsA) and the cell division component MreD. Such novel distribution of proteins complexes can be explained mainly as a by-product of the energy cost of bending that potential complexes exert on the membrane, and the geometric constraints imposed by the latter. A model based on such basic

## Significance

**The fundamental processes of life are organized and based on common basic principles. Molecular organizers, often interacting with the membrane, capitalize on cellular polarity to precisely orientate essential processes. The study of organisms lacking apparent polarity or known cellular organizers (e.g., the bacterium *Staphylococcus aureus*) may enable the elucidation of the primal organizational drive in biology. How does a cell choose from infinite locations in its membrane? We have discovered a structure in the *S. aureus* membrane that organizes processes indispensable for life and can arise spontaneously from the geometric constraints of protein complexes on membranes. Building on this finding, the most basic cellular positioning system to optimize biological processes, known molecular coordinators could introduce further levels of complexity.**

Author contributions: J.G.-L., F.W., and S.J.F. designed research; J.G.-L., F.W., X.M., L.W., R.R.C., J.K., H.C., and R.G. performed research; J.G.-L., F.W., and S.J.F. analyzed data; and J.G.-L., R.G., and S.J.F. wrote the paper.

The authors declare no conflict of interest.

This article is a PNAS Direct Submission.

Freely available online through the PNAS open access option.

Data deposition: The sequence reported in this paper has been deposited in the European Nucleotide Archive, www.ncbi.nlm.nih.gov/bioproject/PRJEB11829 (accession no. PRJEB11829).

[1]Present address: School of Medicine and Dentistry, College of Clinical and Biomedical Sciences, University of Central Lancashire, Preston PR1 2HE, United Kingdom.

[2]Present address: Unilever Future Leader Programme, Unilever R&D, Sharnbrook, Bedford MK44 1LQ, United Kingdom.

[3]Present address: Centre for Inflammation Research, College of Medicine and Veterinary Medicine, University of Edinburgh, Edinburgh EH16 4TJ, United Kingdom.

[4]To whom correspondence may be addressed. Email: s.foster@sheffield.ac.uk or ramin.golestanian@physics.ox.ac.uk.

This article contains supporting information online at www.pnas.org/lookup/suppl/doi:10.1073/pnas.1509557112/-/DCSupplemental.

MICROBIOLOGY

properties offers a new fundamental organizing framework in nondifferentiating coccal bacteria such as *S. aureus*, and may be one of the early cues that dictates the position of a target protein in the ensemble of proteins (22).

## Results and Discussion

**PlsY Is an Essential Protein with a Patterned Distribution in the Membrane.** PlsY is an acyltransferase required for the indispensable process of phospholipid biosynthesis, and highly conserved across bacteria (23, 24). We show that PlsY is essential for the growth of *S. aureus*, demonstrated by the creation of a conditional lethal strain (*SI Appendix*, Fig. S1 *A* and *B*). PlsY-depleted cells exhibit misplaced cell division septa, altered cell wall morphology, and defective cytokinesis, suggesting a problem in cell division (Fig. 1 *A–D* and *SI Appendix*, Fig. S1*F*). To examine the link between PlsY and cell cycle progression, we studied the distribution of divisome proteins EzrA and PBP2. EzrA forms a septal ring at the midplane of the cell and was found at unexpected division planes when cells are depleted for PlsY (Fig. 1 *E–G* and Movie S1) (25, 26). PBP2, a septal protein responsible for cell wall biosynthesis at the site of division (27), was also delocalized (*SI Appendix*, Fig. S2), suggesting PlsY involvement in septum placement and/or division progression.

A chromosomally encoded and functional PlsY–GFP fusion under the control of the *plsY* promoter demonstrated septal localization, but also distributed in a pattern of foci around the membrane throughout the cell cycle (Fig. 2 *A–C*, *SI Appendix*, Figs. S3–S5, and Movie S2). Immunoblot and FACS analysis demonstrated that PlsY is membrane associated (*SI Appendix*, Fig. S6), and *plsY* repression led to a decrease of PlsY (*SI Appendix*, Fig. S1 *C–E*).

The fluorescent translational fusion reporter data were supported by immunofluorescence microscopy observations of PlsY distribution, which also revealed a pattern (Fig. 2*D* and *SI Appendix*, Fig. S7*A*), and optical sectioning of fluorescent or immunolabeled PlsY that showed a 3D distribution of foci (*SI Appendix*, Fig. S3 and Movie S3). The pattern was present in both fixed and unfixed samples, demonstrating that the observed pattern is not an artifact of the sample preparation procedure (*SI Appendix*, Fig. S8*A*). CdsA, a CDP-diacylglycerol synthase

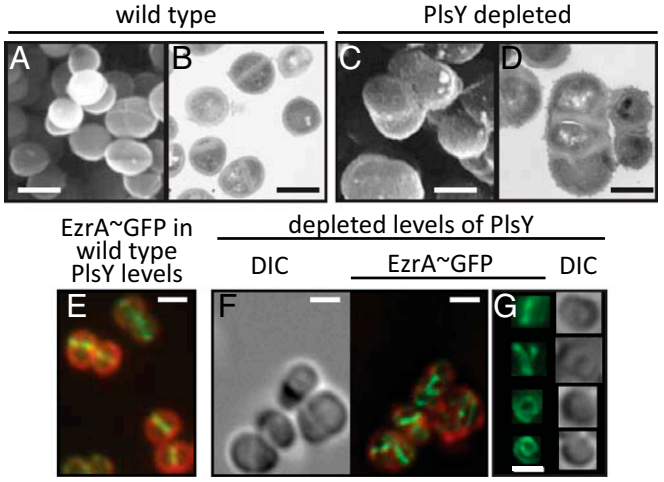


**Fig. 1.** Scanning (*A* and *C*) and transmission (*B* and *D*) electron micrographs of PlsY-depleted *S. aureus* JGL166 (*C* and *D*) reveal aberrant cellular morphologies compared with wild-type cells (*A* and *B*). (*E–G*) Fluorescence microscopy of the cell division-related EzrA protein tagged with GFP (green) reveals its septal location in wild-type cells (*E*); cell membrane is stained with Nile red (red). In contrast, EzrA–GFP is delocalized in the absence of PlsY (*F* and *G*). DIC, differential interference contrast microscopy. (Scale bars, 1 μm.)

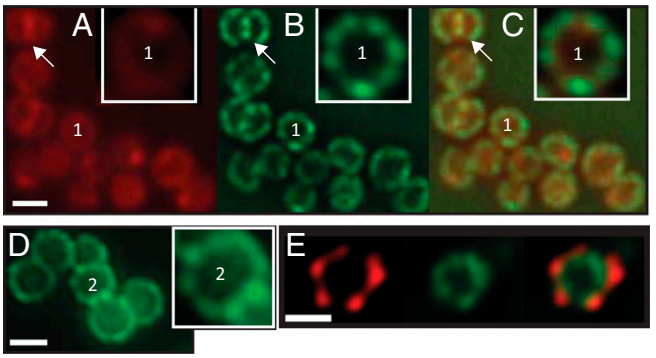


**Fig. 2.** (*A–C*) PlsY localizes to the cell division site (see arrow) but also distributes in a pattern in the membrane of *S. aureus* whether detected by GFP labeling [*B* and *C*, counterstained with Nile red (*A*) or immunolabeling with α-731 antibody (*D*). (*E*) CdsA (GFP labeled, green) has a similar distribution pattern to PlsY and colocalizes with immunolabeled PlsY (red). (Scale bars, 1 μm.)

downstream of PlsY in the glycerophospholipid biosynthesis pathway, localized in a similar pattern and colocalized with PlsY (Fig. 2*E*, *SI Appendix*, Figs. S7*C* and S8*B*, and Movies S4–S6), whereas other membrane proteins did not (e.g., YmdA and SecY; *SI Appendix*, Fig. S7*B*). Consistent with those observations, PlsY and CdsA also showed a weak interaction in a bacterial two-hybrid analysis (BACTH; *SI Appendix*, Fig. S9). To confirm interaction between both components at the molecular level in their natural environment, we implemented a FRET-based system in *S. aureus* using fluorescent protein fusions. A donor bleaching strategy was applied and revealed a specific interaction between PlsY and CdsA (*SI Appendix*, Fig. S10). To our knowledge, these are the first pieces of evidence of the suspected colocalization and interaction between the enzymes in this pathway, and support the notion of metabolic channelling. Lipid clusters are also organized with PlsY in the membrane of unfixed cells (*SI Appendix*, Fig. S11). Such a distribution could correspond to the differential accumulation of specific fatty acid species or lipid conformations in the membrane (28).

**MreD Is Needed for the Formation of a Supramolecular Structure in the Membrane.** PlsY and/or CdsA seemed unlikely candidates as organizers of the patterned distribution, as did FtsZ, despite its link to the localization of phospholipid synthases (29). The MreBCD complex in rod-shaped bacteria localizes along the membrane, acting as a spatial organizer of various processes (7, 9, 30–33). In *Escherichia coli*, MreB (an actin-like molecule) is required to regulate phospholipid and membrane biosynthesis (31). However, MreB is missing in *S. aureus* and other coccal cells, whereas MreC and MreD are present (9).

*S. aureus* deprived of MreC grew identically to the parent, whereas lack of MreD or MreCD led to a growth defect with larger cells of abnormal morphology (Fig. 3 *A–C* and *SI Appendix*, Figs. S12 and S13), reminiscent of the PlsY-depleted phenotype. The lack of an apparent phenotype for the single *mreC* mutation was interesting given its importance in other organisms (34). Genome sequencing of two individual *mreC* mutants revealed one single nucleotide polymorphism in each strain leading to an amino acid substitution (*SI Appendix, Whole Genome Sequencing*). However, those substitutions seem unlikely candidates to justify the lack of an *mreC* phenotype. Loss of MreD can be complemented by ectopic expression of the *mreD* gene (*SI Appendix*, Fig. S13 *F* and *G*). MreD is required for the observed pattern of PlsY (cf. Fig. 2 *B* and *D* with Fig. 3*D* and *SI Appendix*, Fig. S14*A*) and the characteristic placement of EzrA (cf. Fig. 1*G* with Fig. 3*E*, *SI Appendix*, Fig. S14*B*, and Movie S7); this is consistent with the immunodetection of a MreD–GFP fusion that revealed a

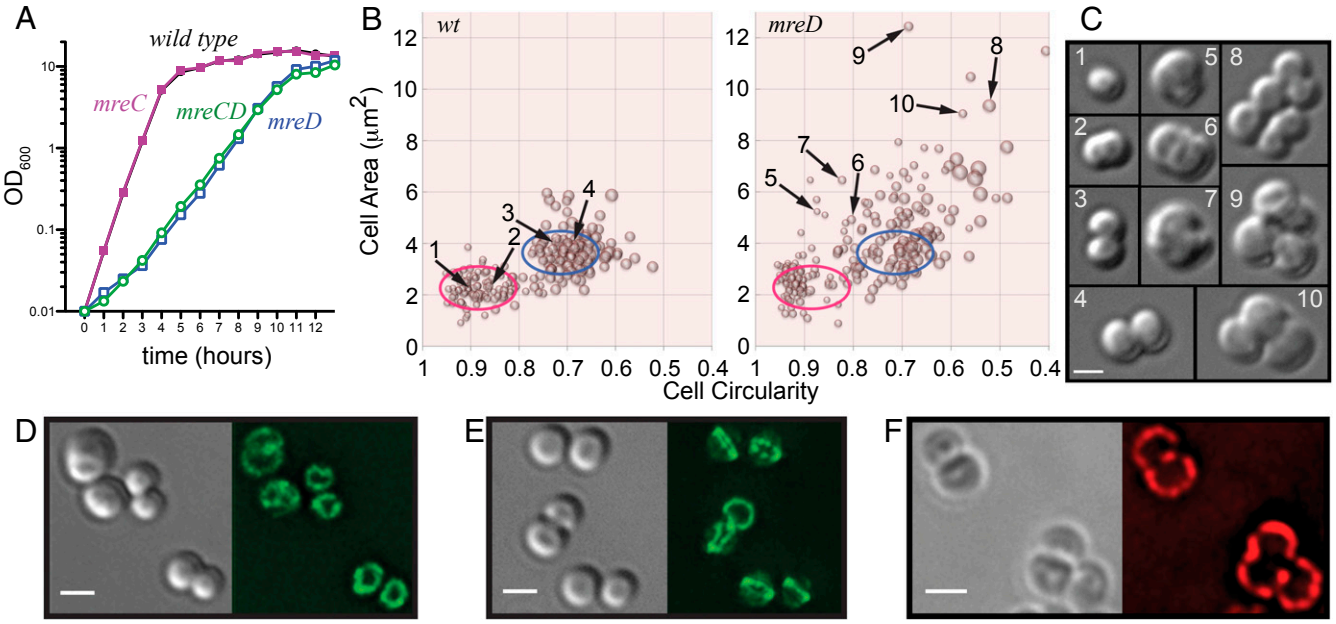


**Fig. 3.** Role of MreD in cell growth and morphology. (*A*) Growth of *S. aureus* SH1000 wild type (●, black), *mreC* deletion mutant (strain SJF4098; ■, pink), *mreD* deletion mutant (strain SJF2976; □, blue), and *mreCD* deletion mutant (strain SJF2625; ○, green). (*B*) Cell size distribution in SH1000 ($n = 235$) and *mreD* mutant (strain SJF2976; $n = 262$) populations of *S. aureus* at $OD_{600} = 0.5–0.8$. Pink ellipse encloses single cells; blue ellipse encloses normally dividing cells. Cell sizes >4.5 μm$^2$ correspond to single, dividing, or clusters of cells of abnormally large size. Two shape descriptors have been used to illustrate cell morphology: cell circularity (*x* axis of the graphs) and cell roundness (illustrated by the diameter of the symbols). (*C*) Examples of the cell categories plotted in Fig. 3*B*. MreD depletion in *S. aureus* leads to the delocalization of GFP-tagged PlsY (*D*) and EzrA (*E*) even in cells with wild-type morphology. (*F*) Immunolocalization of MreD–GFP with anti-GFP antibodies reveals a distribution of MreD in the *S. aureus* membrane similar to PlsY. (Scale bars, 1 μm.)

localization pattern equivalent to PlsY and CdsA (Figs. 2 *B* and *D* and 3*F* and *SI Appendix*, Figs. S3 and S15). BACTH analysis also showed protein–protein interactions between MreD and CdsA (*SI Appendix*, Fig. S9). Similarly, FRET provided supporting evidence of the interaction between MreD and PlsY (*SI Appendix*, Fig. S10).

**Spontaneous Formation of a Patterned Distribution of Protein Complexes in the Membrane.** Without cytoskeletal components, how might MreD, PlsY, and CdsA adopt a pattern in the membrane? Their distribution could arise from the interplay between the potential complex they contribute to and the geometric constraints imposed on the membrane, doing what cellular organizers do, but spontaneously, and leading the way. If the integral membrane protein complex inflicts a sufficiently large local curvature on the membrane, a random distribution would be frustrated due to the high bending energy cost that results from accommodating the complexes across the membrane. This mechanism of protein organization can account for pattern formation of FtsZ in liposomes (35, 36), and is also consistent with the sensing of 2D membrane geometry by the Min system (37).

The apparently spherical membrane of *S. aureus* and any surface deformation can be expressed in spherical coordinates as $\mathbf{R}(\theta,\varphi) = R\,[1 + u(\theta,\varphi)]\hat{\mathrm{r}}$, where $R$ is the radius of the unperturbed sphere, $u(\theta,\varphi)$ describes the surface deformations, and $\hat{\mathrm{r}}$ is the radial unit vector. The distribution of the protein complexes across the membrane is described with the surface number density $\rho(\theta,\varphi) = \rho_0\,[1 + \psi(\theta,\varphi)]$. We assume that each protein complex covers a patch of area $a_0$ and interacts with the membrane geometry by imposing a spontaneous curvature $H_p$ at its location. A free energy functional for the system can be written as the sum of three contributions $\mathcal{F} = \mathcal{F}_b + \mathcal{F}_d + \mathcal{F}_t$; this comprises a bending energy contribution, $\mathcal{F}_b = \kappa/2 \int dA[H^2 - 2H_p\rho a_0 H]$, due to membrane deformation, a contribution due to density fluctuations of the diffusing protein complexes of the form $\mathcal{F}_d = 1/2\chi \int dA[\xi^2(\nabla\psi)^2 + \psi^2]$ that originates from their entropy of mixing, and a harmonic potential $\mathcal{F}_t = kR^2/2 \int dA u^2$ that results from the tethering of the membrane to the vicinity of the cell wall and the turgor pressure. Here, $\kappa$ is the bending rigidity, $H/2$ is the mean curvature, $\chi$ is the compressibility and $\xi$ is the correlation length of the density fluctuations, and $k$ is an effective spring constant (per unit area) representing the confinement potential. Using this free energy, we can define the governing dynamical equations for $u(\theta,\varphi)$ and $\psi(\theta,\varphi)$, which involve the corresponding mobility (transport) coefficients $L_u$ and $L_\psi$ (*SI Appendix*, Fig. S16 and Fig. 4*A*). Keeping the leading order in deformation and density fluctuations, and using expansion in spherical harmonics $Y_{\ell m}(\theta,\varphi)$ for both fields, a linear stability analysis can be performed to find the growth rates of the characteristic modes of the system. It is convenient to group the many parameters in the system into the dimensionless variables $K = kR^4/\kappa$, $M = L_\psi/(\kappa L_u \chi)$, $P = \xi^2/R^2$, and $W = \kappa\chi\rho_0^2 a_0^2 H_p^2$.

Fig. 4*B* shows the relevant growth rate $\lambda_+$ in units of $\kappa L_u/R^2$ as a function of the mode number $\ell$, at selected values of $K$, $M$, and $P$ for $W = 1$. It shows that $\lambda_+$ acquires a positive value (Fig. 4*C*) for the $\ell = 8$ mode, which means that this mode becomes unstable. The instability in the intermediate $\ell = 8$ mode develops as the parameter $W$ is changed from 0.8 to 1 (Fig. 4*D*), leading to the development of slowly growing patterns that are linear combinations of the $Y_{8m}(\theta,\varphi)$ for different values of $m$, which could lead to eight foci in a cross-section of the sphere (Fig. 4*E*). This example demonstrates that patterns such as those observed (Figs. 2 *B–E*, 3 *F* and *G*, and 4 *C* and *D*, *SI Appendix*, Figs. S7 *A* and *C*, S8 *A* and *B*, and S11*B*, and Movies S3–S6) can be generated as a result of such intermediate wavenumber instability.

Assuming that the protein complexes are in the dilute regime—namely, $\rho a_0 \ll 1$, we can estimate the compressibility as $\chi \approx 1/(k_B T \rho_0)$ (38), and write the coupling parameter as

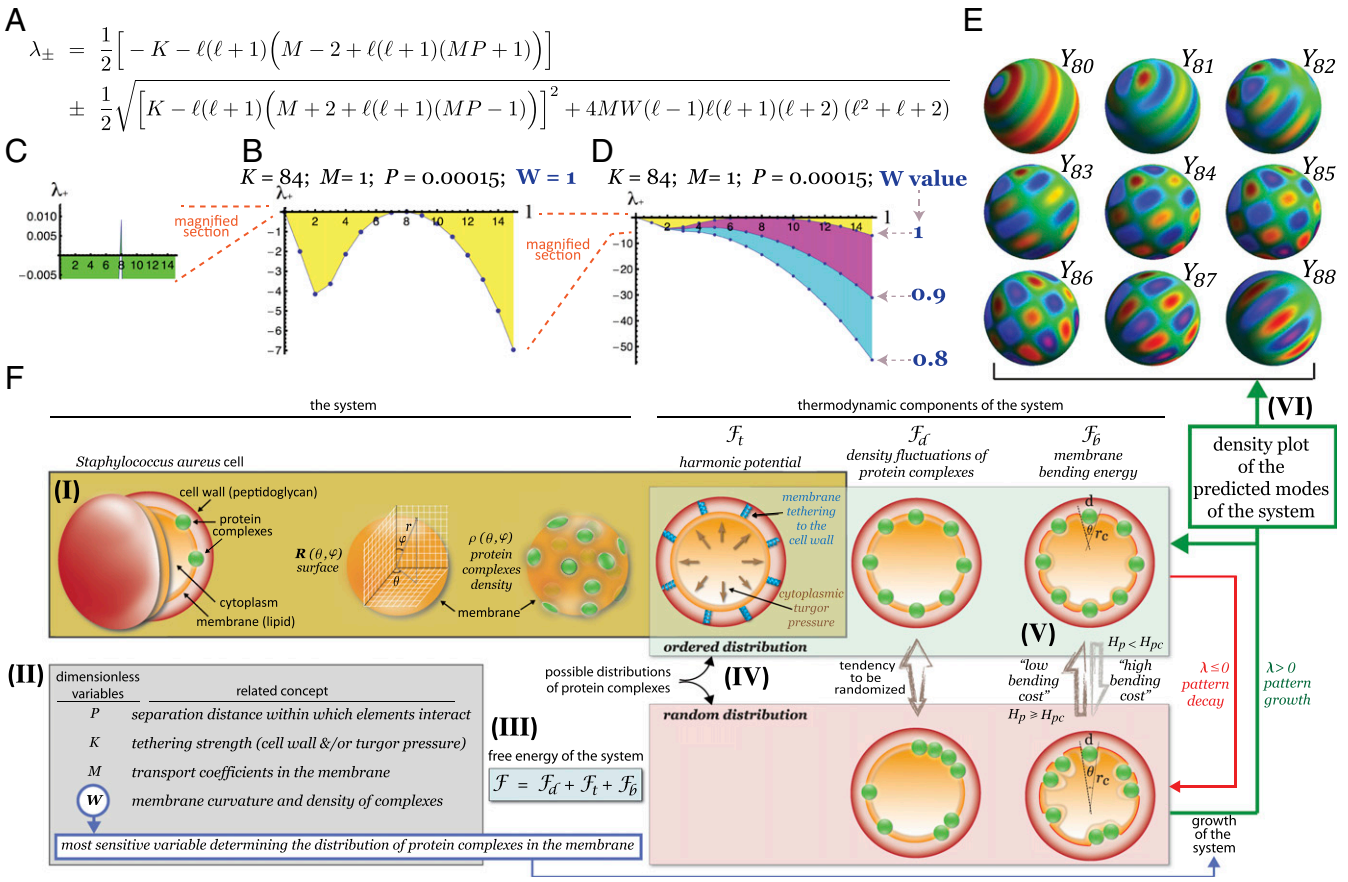


**Fig. 4.** (*A*) Calculated formula of the growth of the system as a function of its modes (l) and the adimensional variables *K*, *P*, *M*, and *W* (*SI Appendix*, Fig. S16). (*B*) The growth rate $\lambda+$ as a function of the mode number *l*, corresponding to $K = 84$, $M = 1$, $P = 0.00015$, and $W = 1$; a magnified section of the latter (*C*) shows that the $l = 8$ mode becomes unstable. (*D*) Instability is exquisitely sensitive to *W* but not to the other variables (*SI Appendix*, Fig. S17). (*E*) Density plots of the real parts of various spherical harmonics $Y_{8m}(\theta, \varphi)$ for different values of *M*. (*F*) See extended explanation in *SI Appendix*, Fig. S17. (I) The bacterial membrane (e.g., *S. aureus* membrane) is a lipid-based surface, under cytoplasm-induced turgor pressure and tethered to the cell wall, which contains protein complexes whose distribution is a 3D phenomenon that can be defined by a mathematical function (*SI Appendix*, Fig. S16). (II) The latter depends on multiple independent variables that can be grouped into dimensionless variables (*P*, *K*, *M*, and *W*) for convenience. (III) This enables one to solve the differential equations corresponding to the various components $(\mathcal{F}_b + \mathcal{F}_d + \mathcal{F}_t)$ of the overall free energy of the system ($\mathcal{F}$). The *P*, *K*, *M*, and *W* variables do not directly correspond to biological variables, but they relate to them in terms of controlling the relative competition between the energy contributions; *K* relates to $\mathcal{F}_t$ vs. $\mathcal{F}_b$, *P* and *M* relate to $\mathcal{F}_d$, and *W* relates to $\mathcal{F}_d$ vs. $\mathcal{F}_b$. (IV and V) The solutions to the equation are two functions $\lambda_+$ and $\lambda_-$, representing the growth ($\lambda > 0$; pattern formation of protein complexes) or decay ($\lambda < 0$ and $\lambda = 0$; random distribution of protein complexes) in the membrane. A combination of selected values of *K*, *P*, *M*, and *W* (Fig. 4 *B*–*D*) as a function of the characteristic modes of the system (l) results in positive $\lambda+$ (*SI Appendix*, Figs. S16 and S17). Linear analysis (Fig. 4 *B*–*D*) reveals *W* as the key variable determining the distribution of protein complexes. Hence, the presence of a protein complex in the membrane induces a membrane deformation that results in localized membrane curvature ($H_p$) and will entail a bending cost. If the curvature is larger than a critical threshold ($H_{pc}$), it will result in a system that will enable the growth of patterns. If $H_p < H_{pc}$, the resulting system will lead to the decay of patterns. (VI) The separation of variables into spherical coordinates leads to spherical harmonics of the form $[Y_{\ell m}(\theta, \varphi)]$ (Fig. 4*E*) that can be represented as a density plot.

$W \approx (\kappa/k_B T)\rho_0 a_0^2 H_p^2$. A critical threshold $W_c \approx 1$ thus means that the pattern forms when the spontaneous curvature of the protein complex is larger than a critical value—namely,

$$H_p > H_{pc} \approx \left(\frac{k_B T}{\kappa \rho_0 a_0^2}\right)^{\frac{1}{2}}. \quad [1]$$

Considering the characteristic values of $\kappa/k_B T \sim 100$ and $\rho a_0 \sim 0.01$, we find a critical radius of curvature of the order of the lateral size of the protein complex. *SI Appendix*, Fig. S17 illustrates the robustness of the model with respect to the choice of the parameters. We choose reasonable values for the parameters, but show that changing them does not alter the main features of our linear stability analysis, which only depend sensitively on *W*, which is essentially controlled by the curvature imposed on the membrane by the protein complex. A simple graphic explanation of the model is presented in Fig. 4*F* and *SI Appendix*, Fig. S17.

## Conclusion

The model of cell organization based on molecular scale self-organization, emerging spontaneously and without guidance, offers a new fundamental organizing framework for proteins in coccal organisms, such as *S. aureus*; this establishes an early cue that dictates the position of a target protein in the overall ensemble (22). The competition between the various forces at play leading to the ordered distribution of protein complexes in the membrane constitutes in essence an intrinsic amplifier that can act as a sensitive switch enabling the fine-tuning of important cellular processes. Less-favorable $\lambda$ values leading to different protein patterns or pattern decay could still be preferentially selected as an expansion of the model; this could occur through the anisotropy introduced by forces generated by molecular structures (e.g., cell curvature) (39) or by the recruitment of specific proteins to subcellular sites, such as the assembly of penicillin binding proteins by MreB or FtsZ (40). Such molecular networks may form a basic system to coordinate life.

In eukaryotes, membrane partitioning is a well-described process with features at different length scales (41). In prokaryotes, it would also be envisaged that multiple mechanisms are at play, resulting in the coordination of processes from the molecular to the cellular level. The ability to colocalize members of the same macromolecular biosynthesis pathway provides a dynamic mechanism to permit efficient metabolism. Phospholipid biosynthesis involves complex intermediates and potential substrate channelling between enzymes, which would require their colocalization. The development of FRET in *S. aureus* has provided the experimental framework to test juxtaposition of proteins in their native membrane setting, which has shown the interaction between PlsY and CdsA. It will be of great interest to determine the localization pattern of other phospholipid biosynthesis enzymes in the pathway and to extend this to further proteins involved in other metabolic processes and beyond. It may be that such protein assemblies generate localized physiobiochemical environments propagating effects to other membrane components in the same or different processes. The observation of apparent differential partitioning of PlsY and a lipid dye in the membrane supports such a hypothesis (*SI Appendix*, Fig. S11).

It has previously been shown that MreB, in rod-shaped cells, acts as a guidance mechanism for multiple biosynthetic components (11). However, the roles of MreC and MreD have remained more obscure. Here we find an important role for MreD in growth in an organism lacking MreB. Deletion of *mreD* results in pleiotropic effects, and we suggest that in rods, MreB may spatially constrain MreD, but it is MreD that is itself a key player in the actual coalescence of molecules. In *S. aureus* we also see evidence of cellular morphology effects on MreD-associated processes during the cell cycle. Thus, other spatiotemporal cues will be brought into play to allow coordination during growth and division. We have hypothesized that cell wall peptidoglycan architectural features can provide a template for division site recognition (42). It is likely a combination of intrinsic properties of proteins, such as MreD, that may provide localized perturbation to the membrane, coupled with larger scale morphological features derived from other cellular components and morphological dynamics generated from apparent cytoskeletal elements (such as FtsZ) that determine the overall mapping of membrane components. Such a dynamic accumulation of cues optimizes cellular reactions within a given environment.

In a drive to understand the basis of life, a key goal is the ability to assemble a protocell capable of self-assembly (43). Unraveling the mechanisms underpinning such assembly is crucial. Our observations provide a novel and basic organizational drive of proteins in membranes, and catalyze further research to determine their behavior in vitro and in vivo to understand patterning in a lipid environment and in the interplay within and between cellular processes. The mathematical model presented here gives a theoretical framework to be tested and to begin to predict the behavior of components underpinning life.

## Materials and Methods

This section briefly recapitulates the data analysis methods. A detailed description of methods can be found in *SI Appendix*. IPTG-inducible expression constructs of *plsY* in single copy in the staphylococcal chromosome, as well as *mreC* and *mreD* deletion strains, were made through allelic replacement by double crossover recombination. The process involved the use of episomal vectors with temperature-sensitive replicons, initially constructed in *E. coli* (TOP10), followed by passaging of the resulting constructs through a restriction-deficient strain (*S. aureus* RN4220) and subsequent transduction-mediated integration into the final test strain (*S. aureus* SH1000). The *mreD* complementation plasmid was based on *S. aureus* replication-stable episomes. A similar procedure was followed to generate GFP-transcriptional fusions but mediated through single crossover recombination that resulted in an intact copy of the gene of interest under the control of the regulatable promoter Pspac, and another copy of the gene fused to GFP under the control of the native promoter of the gene of interest. The rest of the techniques, including protein and antibody production, immunolabeling, epifluorescence and electron microscopy preparation, flow cytometry analysis, bacterial two-hybrid analysis, FRET, and cell fractionation, were performed according to standard techniques optimized to our project. Imaging was undertaken with a DeltaVision RT Deconvolution microscope (Applied Precision) linked to an Olympus IX70 microscopy system (Olympus U-RFL-T and IX-HLSH100 lamps, and Olympus UPlanApo 100×/1.35 oil iris lens), with SoftWoRx 3.5.1 software. Cell enumeration and perimeter, major axis, and minor axis measurements were performed using ImageJ 1.46o.

**ACKNOWLEDGMENTS.** The work was funded by the Biotechnology and Biological Sciences Research Council, UK.

1. Barry RM, Gitai Z (2011) Self-assembling enzymes and the origins of the cytoskeleton. *Curr Opin Microbiol* 14(6):704–711.
2. Cabeen MT, Jacobs-Wagner C (2010) The bacterial cytoskeleton. *Annu Rev Genet* 44: 365–392.
3. Marston AL, Errington J (1999) Selection of the midcell division site in *Bacillus subtilis* through MinD-dependent polar localization and activation of MinC. *Mol Microbiol* 33(1):84–96.
4. Rowlett VW, Margolin W (2013) The bacterial Min system. *Curr Biol* 23(13):R553–R556.
5. Carballido-López R, Formstone A (2007) Shape determination in *Bacillus subtilis*. *Curr Opin Microbiol* 10(6):611–616.
6. Daniel RA, Errington J (2003) Control of cell morphogenesis in bacteria: Two distinct ways to make a rod-shaped cell. *Cell* 113(6):767–776.
7. Figge RM, Divakaruni AV, Gober JW (2004) MreB, the cell shape-determining bacterial actin homologue, co-ordinates cell wall morphogenesis in *Caulobacter crescentus*. *Mol Microbiol* 51(5):1321–1332.
8. Formstone A, Errington J (2005) A magnesium-dependent *mreB* null mutant: implications for the role of *mreB* in *Bacillus subtilis*. *Mol Microbiol* 55(6):1646–1657.
9. Jones LJ, Carballido-López R, Errington J (2001) Control of cell shape in bacteria: Helical, actin-like filaments in *Bacillus subtilis*. *Cell* 104(6):913–922.
10. van den Ent F, Amos LA, Löwe J (2001) Prokaryotic origin of the actin cytoskeleton. *Nature* 413(6851):39–44.
11. Errington J (2015) Bacterial morphogenesis and the enigmatic MreB helix. *Nat Rev Microbiol* 13(4):241–248.
12. Thanbichler M (2010) Synchronization of chromosome dynamics and cell division in bacteria. *Cold Spring Harb Perspect Biol* 2(1):a000331.
13. Errington J (2013) L-form bacteria, cell walls and the origins of life. *Open Biol* 3(1): 120143.
14. Leaver M, Domínguez-Cuevas P, Coxhead JM, Daniel RA, Errington J (2009) Life without a wall or division machine in *Bacillus subtilis*. *Nature* 457(7231):849–853.
15. Mercier R, Kawai Y, Errington J (2014) General principles for the formation and proliferation of a wall-free (L-form) state in bacteria. *eLife* 3:3.
16. Strahl H, Hamoen LW (2012) Finding the corners in a cell. *Curr Opin Microbiol* 15(6): 731–736.
17. Barák I, Muchová K (2013) The role of lipid domains in bacterial cell processes. *Int J Mol Sci* 14(2):4050–4065.
18. Lenn T, Leake MC, Mullineaux CW (2008) Clustering and dynamics of cytochrome bd-I complexes in the *Escherichia coli* plasma membrane in vivo. *Mol Microbiol* 70(6): 1397–1407.
19. Tzagoloff H, Novick R (1977) Geometry of cell division in *Staphylococcus aureus*. *J Bacteriol* 129(1):343–350.
20. Margolin W (2009) Sculpting the bacterial cell. *Curr Biol* 19(17):R812–R822.
21. Zapun A, Vernet T, Pinho MG (2008) The different shapes of cocci. *FEMS Microbiol Rev* 32(2):345–360.
22. Shapiro L, McAdams HH, Losick R (2009) Why and how bacteria localize proteins. *Science* 326(5957):1225–1228.
23. Chaudhuri RR, et al. (2009) Comprehensive identification of essential *Staphylococcus aureus* genes using transposon-mediated differential hybridisation (TMDH). *BMC Genomics* 10:291.
24. Lu YJ, et al. (2006) Acyl-phosphates initiate membrane phospholipid synthesis in Gram-positive pathogens. *Mol Cell* 23(5):765–772.
25. Jorge AM, Hoiczyk E, Gomes JP, Pinho MG (2011) EzrA contributes to the regulation of cell size in *Staphylococcus aureus*. *PLoS One* 6(11):e27542.
26. Steele VR, Bottomley AL, Garcia-Lara J, Kasturiarachchi J, Foster SJ (2011) Multiple essential roles for EzrA in cell division of *Staphylococcus aureus*. *Mol Microbiol* 80(2): 542–555.
27. Pinho MG, Errington J (2003) Dispersed mode of *Staphylococcus aureus* cell wall synthesis in the absence of the division machinery. *Mol Microbiol* 50(3):871–881.
28. Strahl H, Bürmann F, Hamoen LW (2014) The actin homologue MreB organizes the bacterial cell membrane. *Nat Commun* 5:3442.
29. Addinall SG, Holland B (2002) The tubulin ancestor, FtsZ, draughtsman, designer and driving force for bacterial cytokinesis. *J Mol Biol* 318(2):219–236.
30. Soufo HJ, Graumann PL (2003) Actin-like proteins MreB and Mbl from *Bacillus subtilis* are required for bipolar positioning of replication origins. *Curr Biol* 13(21):1916–1920.
31. Bendezú FO, de Boer PA (2008) Conditional lethality, division defects, membrane involution, and endocytosis in *mre* and *mrd* shape mutants of *Escherichia coli*. *J Bacteriol* 190(5):1792–1811.

32. Cowles KN, Gitai Z (2010) Surface association and the MreB cytoskeleton regulate pilus production, localization and function in *Pseudomonas aeruginosa*. *Mol Microbiol* 76(6):1411–1426.
33. Leaver M, Errington J (2005) Roles for MreC and MreD proteins in helical growth of the cylindrical cell wall in *Bacillus subtilis*. *Mol Microbiol* 57(5):1196–1209.
34. Land AD, Winkler ME (2011) The requirement for pneumococcal MreC and MreD is relieved by inactivation of the gene encoding PBP1a. *J Bacteriol* 193(16):4166–4179.
35. Osawa M, Anderson DE, Erickson HP (2008) Reconstitution of contractile FtsZ rings in liposomes. *Science* 320(5877):792–794.
36. Shlomovitz R, Gov NS (2009) Membrane-mediated interactions drive the condensation and coalescence of FtsZ rings. *Phys Biol* 6(4):046017.
37. Schweizer J, et al. (2012) Geometry sensing by self-organized protein patterns. *Proc Natl Acad Sci USA* 109(38):15283–15288.
38. Cai W, Lubensky TC (1995) Hydrodynamics and dynamic fluctuations of fluid membranes. *Phys Rev E Stat Phys Plasmas Fluids Relat Interdiscip Topics* 52(4): 4251–4266.
39. Cabeen MT, et al. (2009) Bacterial cell curvature through mechanical control of cell growth. *EMBO J* 28(9):1208–1219.
40. Claessen D, et al. (2008) Control of the cell elongation-division cycle by shuttling of PBP1 protein in *Bacillus subtilis*. *Mol Microbiol* 68(4):1029–1046.
41. Kusumi A, Suzuki KG, Kasai RS, Ritchie K, Fujiwara TK (2011) Hierarchical mesoscale domain organization of the plasma membrane. *Trends Biochem Sci* 36(11):604–615.
42. Turner RD, et al. (2010) Peptidoglycan architecture can specify division planes in *Staphylococcus aureus*. *Nat Commun* 1:26.
43. Kretschmer S, Schwille P (2014) Toward spatially regulated division of protocells: Insights into the *E. coli* Min system from in vitro studies. *Life (Basel)* 4(4):915–928.